Journal of Molecular Liquids 265 (2018) 585–591

Contents lists available at ScienceDirect

Journal of Molecular Liquids

journal homepage: www.elsevier.com/locate/molliq

Details of charge distribution in stable viral capsid

Elvira Tarasova [a,c,*], Vladimir Farafonov [b], Makoto Taiji [c], Dmitry Nerukh [d]

[a] Immanuel Kant Baltic Federal University, A. Nevskogo str. 14, Kaliningrad 236041, Russian Federation
[b] Department of Physical Chemistry, V.N. Karazin Kharkiv National University, Svobody Square 4, Kharkiv 61022, Ukraine
[c] Laboratory for Computational Molecular Design, RIKEN Center for Biosystems Dynamics (BDR), Building B, 6-2-4 Furuedai, Suita, Osaka 565-0874, Japan
[d] Systems Analytics Research Institute, Department of Mathematics, Aston University, Birmingham B4 7ET, UK

ARTICLE INFO

Article history:
Received 2 April 2018
Received in revised form 25 May 2018
Accepted 5 June 2018
Available online 06 June 2018

ABSTRACT

We present the results of Molecular Dynamics simulations of a viral capsid with the aim to analyse ion distribution on the capsid's surface that defines its stability. Two systems were modelled, a stable capsid with neutralising number of ions and an unstable capsid with low number of ions. For the ion distribution analysis the capsid's structure was identical and fixed in both simulations. It was then released for the stability analysis. The ion distribution demonstrated two types of the local regions on the inner surface of the capsid's wall: highly occupied with chloride ions in both systems despite a largely uniform electrostatic potential everywhere on the surface, and the regions that lose acid. The latter regions are located close to the cracks that are formed when the capsid is destabilised and thus could initiate the collapse of the capsid.

1. Introduction

Recent advances in cryo-EM and X-ray crystallography allow experimental determination of atomistic structure of very large and complex molecular systems such as complete cellular organelles or viruses. As it is only possible to obtain the structure of immobilised molecular objects (embedded in a crystal or frozen), research on the details of their liquid environment at the same molecular scale becomes critically important for utilising the experimental results for more realistic situations resembling the cellular environment.

Whole viruses are particularly attractive from this point of view as they are examples of self-contained complex biological objects spending parts of their lifecycle in isolation from the host cell without any interaction with other biological entities. Aqueous solution is the only external environment required for their existence at these stages of the lifecycle. On one hand, solution with some specific properties (thermodynamic parameters, ion composition, etc.) is needed for a stable virus particle, on the other hand, virus alters the surrounding water in a very specific way that may define the mechanism of the virus stability. Therefore, understanding the details of the molecular properties of the solution is important not only from the academic point of view, but also as a potential route for destabilising the virus (by changing its environment) and, thus, killing the virus.

As the experimental approaches to establishing the structure and dynamics of the solution are much more limited, especially at physiological temperature, Molecular Dynamics (MD) simulations become a valuable tool for studying the aqueous environment of viruses. Recently MD simulations are effectively used for studying the structure, dynamics and properties of whole viruses, in particular viral capsids, which protect the viral genome. These investigations provided details of virus and solution properties that are currently impossible to obtain experimentally, such as permeability of water molecules and ions through the capsid wall [1–4], water molecule diffusion [4, 5], capsid's stability [1, 2, 6], the structure of viral fragments which are missed from experimental data [3, 6, 7], the mechanical properties of the virus particle [8], the swelling of viral capsids [9–11], and others.

To date, one of the most challenging problems experimentally and computationally is the localisation of the genome inside the capsid and its interaction with the capsid. Experimentally, asymmetric packing of the DNA or RNA chain does not allow crystallography to obtain its structure, while the resolution of single-particle cryo-EM is not enough to resolve the atomistic structure of the genome. The lack of reliable experimental information makes it practically impossible to build a reasonable initial structure for MD simulations.

Interesting correlation between the locations of the chloride ions from the solution and the genome molecule has been found by the authors of [12]. They observed that in the absence of the genome the chloride ions occupy the same places next to the inner wall of the capsid as the phosphate groups of the genome. Our previous all-atom MD simulation [6] of an empty porcine circovirus (PCV2) capsid revealed that the number of ions inside the capsid is critical for its stability in the absence of the genome inside. It is known experimentally that the PCV2 capsid can be stable without the genome [13, 14] and its atomistic structure was measured with an X-ray assay [13]. Our results demonstrate that

* Corresponding author at: Immanuel Kant Baltic Federal University, A. Nevskogo str. 14, Kaliningrad 236041, Russian Federation
E-mail address: elvira.tarasova@riken.jp (E. Tarasova).

https://doi.org/10.1016/j.molliq.2018.06.019
0167-7322/

the deficit of the chloride ions next to the inner surface of the capsid destabilises its structure.

The aim of the work reported here is to investigate the molecular details of the ion distribution and to identify which regions of the inner surface should be covered with chloride ions to maintain the integrity of the capsid structure. The main idea is to compare the MD results of a stable capsid and the ones for an unstable capsid. The systems are prepared in such a way that the only difference between them is the number of ions; all other properties, including the structure of the capsid itself are kept identical. We perform a detailed analysis of the ion distribution and reveal critical locations that cause the capsid's destabilisation.

2. Materials and methods

The preparation of the system and the protocols of the MD simulation are given in our previous publications [1, 6]. A protein subunit of PCV2 capsid has been taken from Protein Data Bank (PDB) [15] and reconstructed into full empty capsid with the program VIPERdb [16].

MD simulations were performed using GROMACS [17, 18], VMD program [19] was used for visualisation. The simulations and analysis were carried out in AMBER03 force field with TIP3P water model.

The capsid has the positive charge of +360 e and the charge is distributed disproportionally between the inner and the outer surfaces [6]. With the aim to neutralize this charge we performed two separate procedures of adding the chloride ions inside the capsid and sodium ions outside of it. The quantities were 606 Cl^- and 246 Na^+, because a charge of −606 has been found needed for the complete neutralization of the positive charge of the inner surface. Finally, on the third stage we added 1720 Na^+ and 1720 Cl^- ions randomly scattered across the cell to mimic physiological solution of 0.15 M concentration. This system will be called the natural system (NS). For the preparation of the artificial system (AS), we added one half of the necessary number of the chloride ions inside the capsid, i.e. 300 Cl^-. Because the capsid charge is +360 e, 60 Cl^- were placed to the outer solution instead of Na^+. The same sodium chloride buffer was added as well. Both systems were electroneutral as a whole.

We performed energy minimisation, after that we executed 1 ns MD simulations of the systems with positions of all atoms of the capsid being restrained. During the preparation for the productive run the temperature was gradually increased from 200 K to 300 K [1, 6]. Finally, productive MD simulation was carried out for 10 ns at 300 K. PME method was employed for computing electrostatic interactions, and cut-off with radius 1 nm for van der Waals interactions.

The native structure of the capsid has pores that connect the inside and the outside of the virus. In our previous paper [1] we have found that sodium and chloride ions cannot pass through the pores. However, water molecules could diffuse in both directions. This allowed us to conclude that the PCV2 capsid wall functions as a semipermeable membrane, that is similar to what was shown for a poliovirus capsid [4].

We have performed the analysis of the radial distribution functions (RDFs) of the ions in the solution as a function of the distance from the centre of the capsid for the natural and artificial systems. The analysis was done using the last 200 ps interval of the 1 ns restrained run. We did not use the productive run when the restrains were removed because we were analysing the reasons that later caused the capsid's deformation occurred when the capsid was unrestrained. During 800 ps of the restrained MD run the ions were able to move freely and achieve the equilibrium distribution.

3. Results and discussion

Fig. 1 shows a typical deformation of the capsid in the artificial system with suboptimal number of ions in the interior. We have demonstrated quantitatively that this deformation does not have a tendency to stop and it eventually leads to the formation of large cracks in the capsid's wall that compromise the overall integrity of the virus [6]. We have also shown that this is caused by the lack of negative charge in the layer of the solution adjacent to the inner surface of the capsid that compensates the positive charge of the surface.

A snapshot of the ion distribution in the stable system demonstrates rather dense accumulation of chloride ions next to the inner surface, Fig. 2. This is, of course, expected; however, the quantitative details reveal interesting features of this distribution, in particular when compared to the unstable system. The RDFs of ions as functions of the distance from the capsid's centre of mass (COM) are shown in Fig. 3.

It can be seen that in the capsid with the neutralising number of ions, there is a split peak at ~7 nm, while in the capsid with the low number of ions, this peak is absent. Fig. 2 also gives a hint for explaining this feature: even though the shape of the capsid is close to spherical, it has pronounced internal 'cavities' in the vicinities of the pores. They are formed by the icosahedral shape of the capsid, clearly visible when the atoms beyond the 7.5 nm distance from COM are highlighted (yellow areas in Fig. 5). The number of Cl^- in these 'corners' reach 190 and they are almost completely absent in the unstable system. The peak at ~6 nm is also lower for the unstable capsid, lacking approximately 100 ions.

Sodium ions in both cases are distributed similarly inside the capsid. However, for the natural system, an additional layer of Na^+ ions exists around the outer surface. This could be a consequence of the difference in the total number of Na^+ in the bulk solution (in NS it is higher by 226 than in AS) and their initial distribution, but we believe this is not the case. The total number of Na^+ outside is high for both cases (~1600 in

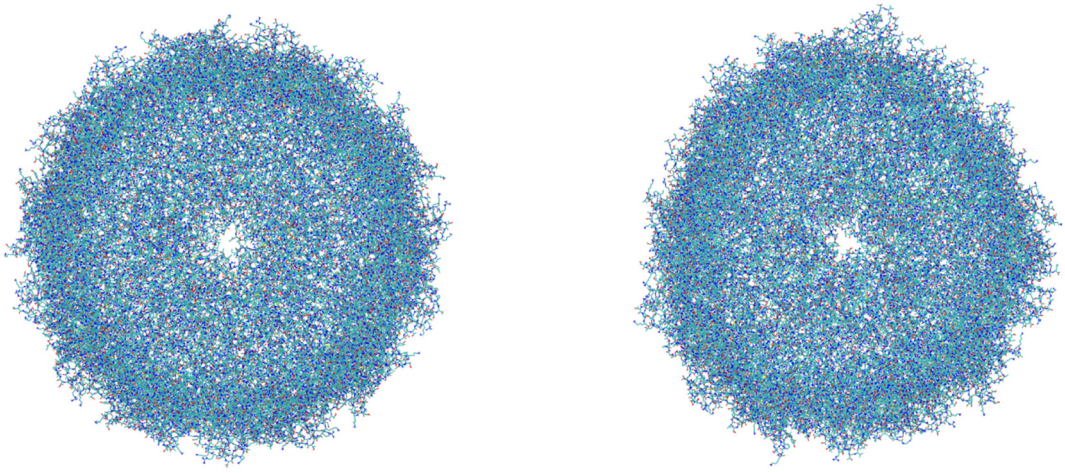

Fig. 1. Stable (left) and deformed (right) capsids; the deformation is progressive leading to the capsid's collapse.

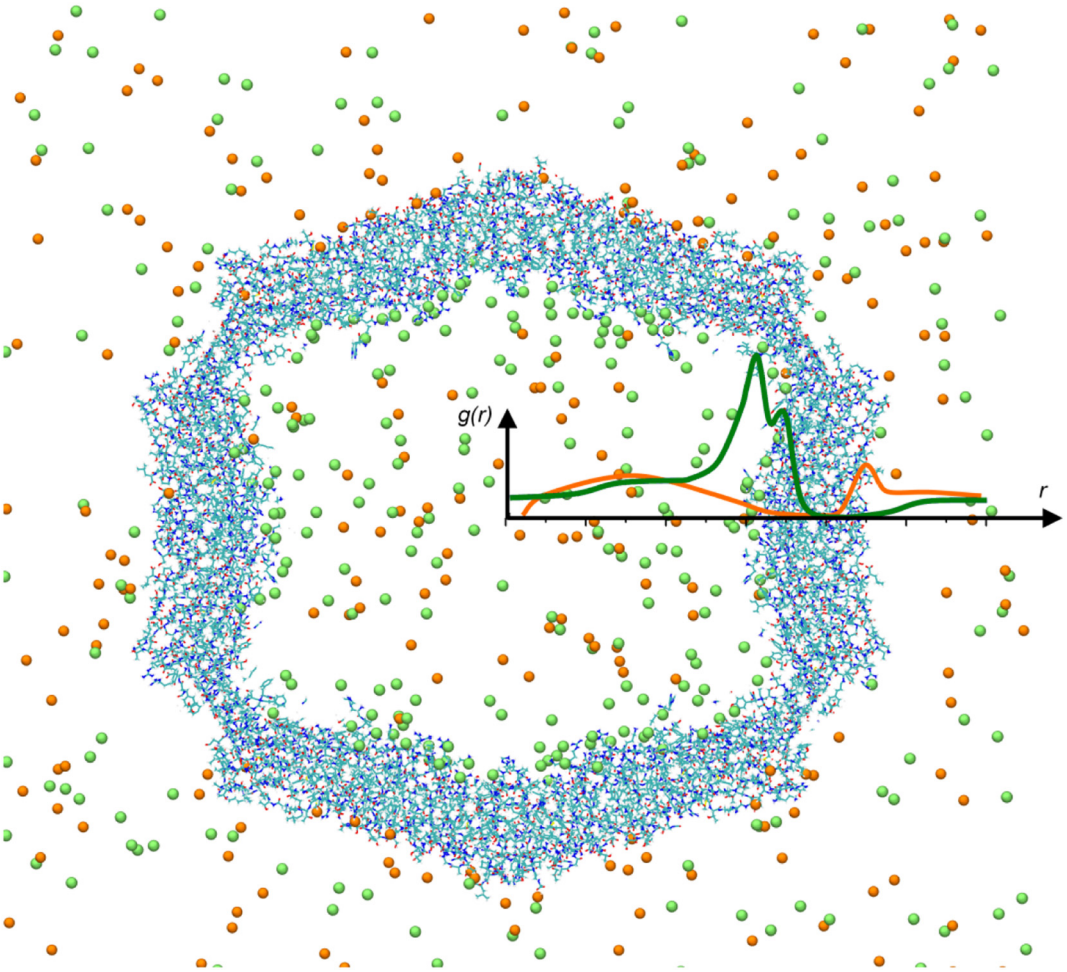

Fig. 2. Schematic illustration of the distribution of Cl^- (green) and Na^+ (orange) ions in the system and RDFs quantifying their concentration as a function of the distance from the capsid's centre of mass. (For interpretation of the references to color in this figure legend, the reader is referred to the web version of this article.)

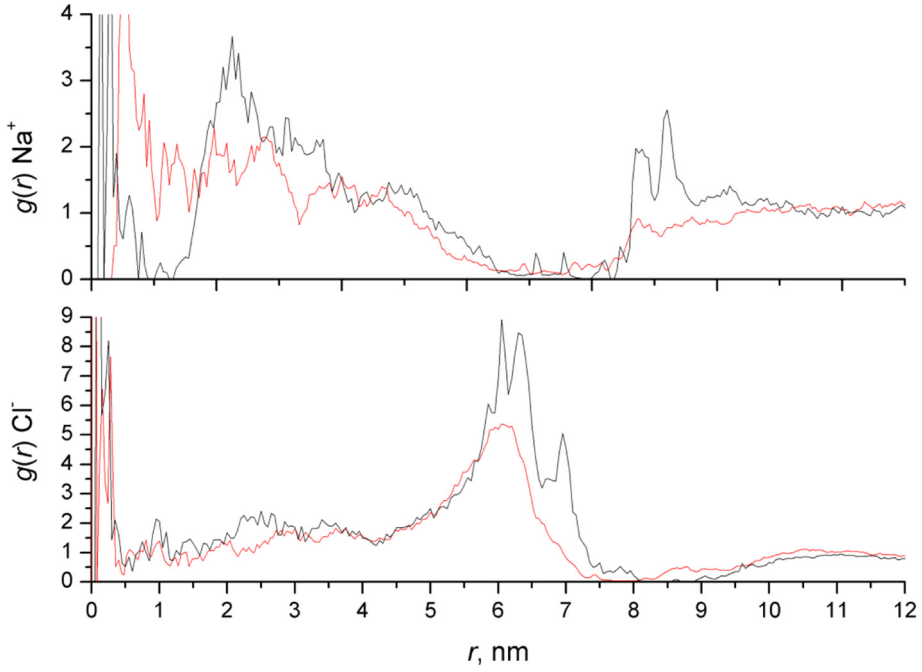

Fig. 3. Radial distribution functions for Na^+ (top) and Cl^- (bottom) ions relative to the capsid's centre of mass; black lines are for the stable capsid, red lines are for the deformed capsid. (For interpretation of the references to col006Fr in this figure legend, the reader is referred to the web version of this article.)

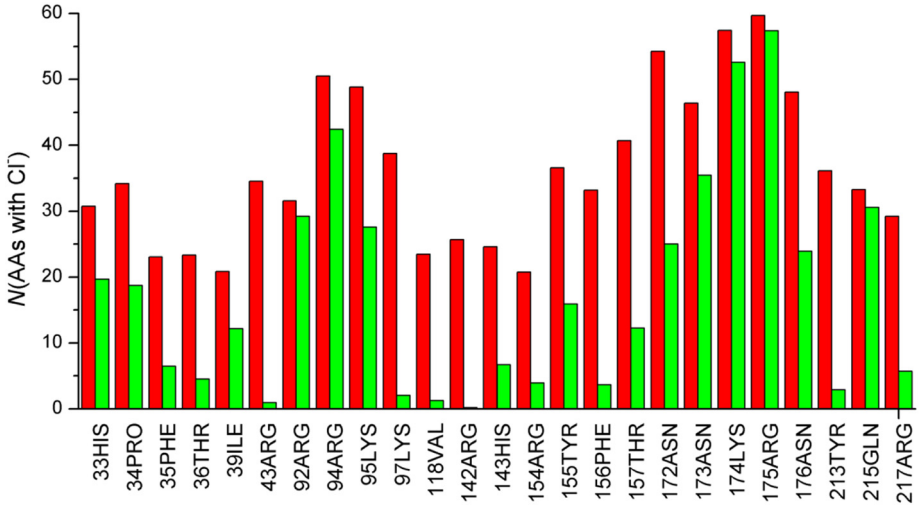

Fig. 4. Number of residues having a Cl^- ion closer than 5 Å; only amino acids having >20 residues contacting with Cl^- in the stable capsid are shown; red – natural system, green – artificial system. (For interpretation of the references to color in this figure legend, the reader is referred to the web version of this article.)

AS), that should be enough to form a layer if needed. Moreover, if necessary, at least a small, thin layer should have been appeared in AS, but there is no evidence of that.

The RDFs quantify the distribution of the ions between spherical layers, they do not show how the ions are distributed within each layer, in particular in the important layers adjacent to the inner surface of the capsid. To analyse the details of the ion accumulation at particular locations of the inner surface, for each amino acid we calculated the average number of residues of this amino acid that have at least one Cl^- ion in its vicinity (within the distance of 5 Å). Evidently, this number changes from 0 (e.g., the amino acid is negatively charged and repulse Cl^-) to 60 (this residue in each of the 60 proteins is in contact with a Cl^- ion). The distributions for both systems (natural and artificial) are shown in Figs. 4, 1S.

For the stable capsid, several amino acids have strikingly high values of this Cl^- occupation: for residues 172(Asn), 174(Lys), and 175(Arg),

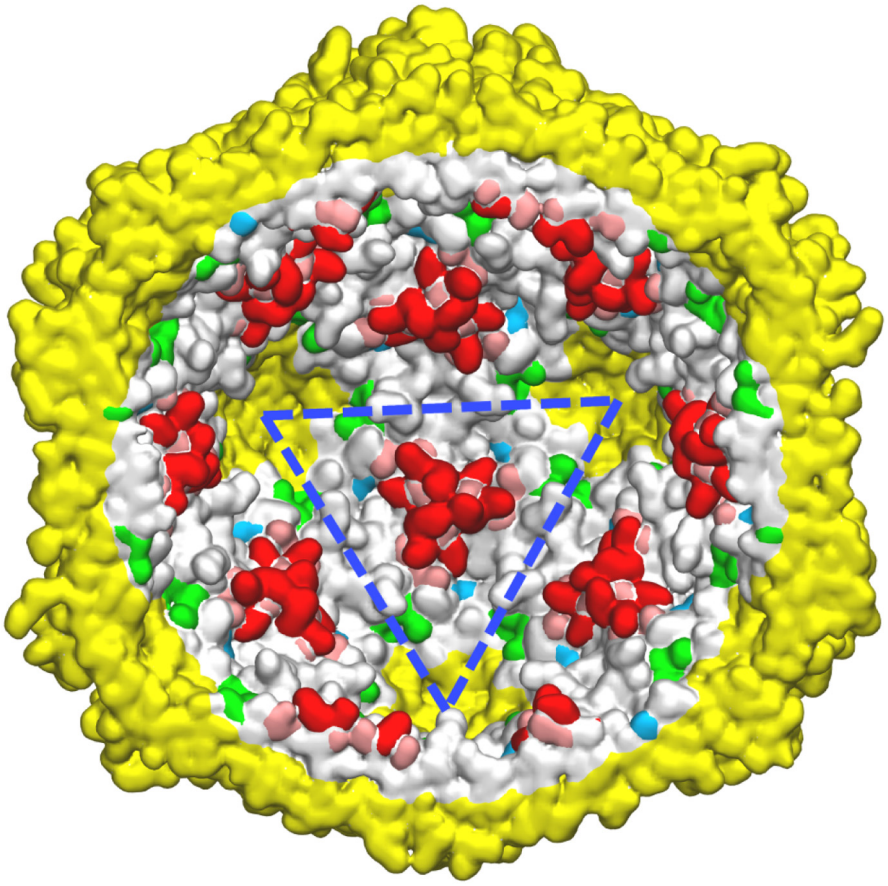

Fig. 5. Half of the capsid revealing the location of the chloride-rich amino acids 172(Asn), 174(Lys), 175(Arg) (red) and 94(Arg), 95(Lys), 173(Asn), 176 (Asn) (pink) and chloride-losing amino acids 43(Arg), 97(Lys), 142(Arg), 213(Tyr) (green) and 118(Val), 156(Phe) (blue); the residues at the distance more than 7.5 nm from the capsid's centre of mass are shown in yellow; one trimer is indicated by the dashed contour. (For interpretation of the references to color in this figure legend, the reader is referred to the web version of this article.)

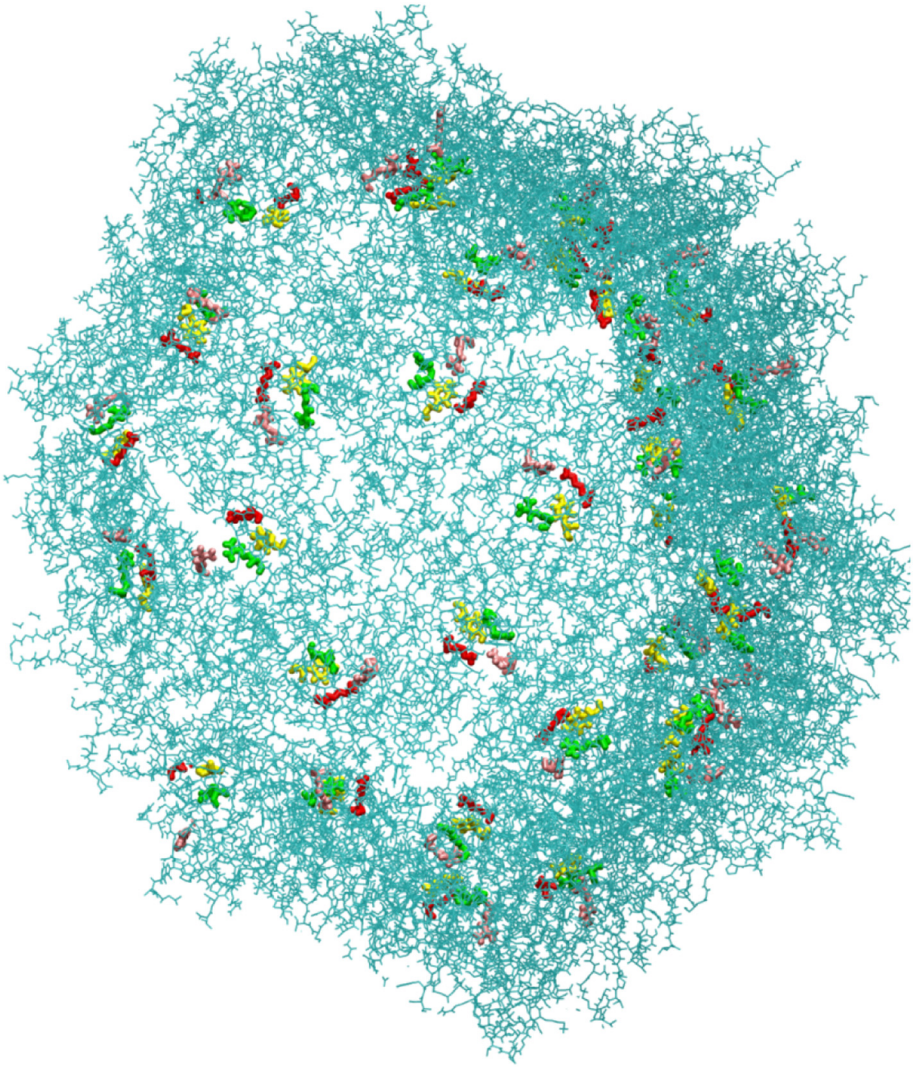

Fig. 6. The half of the deforming capsid after 10 ns of MD simulation. Amino acids 43(Arg), 97(Lys), 142(Arg), and 213(Tyr) are highlighted green, red, pink, and yellow, respectively. (For interpretation of the references to color in this figure legend, the reader is referred to the web version of this article.)

in almost all proteins (≥55 out of 60) each of these amino acids has Cl^- around. Residues 94(Arg), 95(Lys), 173(Asn), and 176(Asn) followed, with the occupation values ≥47 out of 60. Importantly, the occupations of 174(Lys) and 175(Arg) are almost the same in both NS and AS systems. These observations indicate that the described regions are extremely attractive for anions. Therefore they can readily serve as attaching places for the viral genome packed inside the capsid.

The proteins of the capsid form trimers as geometrical units, the capsid is built from them. One of such trimers is indicated in Fig. 5. Interestingly, the 'Cl^- rich' amino acids from the three protein monomers forming a trimer are located very close to each other despite the high positive charge of these amino acids. They are not distributed uniformly on the inner surface of the capsid as it could be expected in order to minimise the mutual electrostatic repulsion. Thus, the presence of the negative charge close to this group of residues is likely to be essential when the trimer is formed. This allows to suggest that the formation of trimers from monomers would be strongly facilitated by the presence of DNA in solution serving as a support by providing the necessary negative charge. We have visualised these chloride-rich areas of the inner surface in Fig. 5.

Another observation from Fig. 4 is that there is a number of residues that lose significantly more chloride ions than others in AS compared to NS. These are residues 43(Arg), 97(Lys), 118(Val), 142(Arg), 156(Phe), 213(Tyr) that also have high occupations in NS but lose almost all chloride ions when going from the stable capsid to the unstable. They are separated in two groups (highlighted in green and blue in Fig. 5) and located on the 'rim' of the cavities containing the pores.

It is difficult to identify one particular area of the capsid where the deformation starts and which triggers its collapse. It seems that a large part of the shell consisting of several proteins folds inwards at some moment. However, there are cases when an obvious crack is formed next to the pore. We have checked the relative location of the crack and the residues that we identified as mostly affected in the unstable system. The result is shown in Fig. 6. Amino acids 43(Arg), 97(Lys), 142(Arg), 213 (Tyr) (highlighted in green in Fig. 5) are located in the crack region, that means that the absence of Cl^- close to them could be the critical factor initiating the destabilisation of the whole capsid.

Finally, we computed the map of the electrostatic potential distribution inside the non-deformed capsid using APBS software [20]. The default settings were used, no 'mobile ions' were added. Water molecules and ions were excluded from computation because their presence would screen the capsid's potential. The obtained map is shown in Fig. 7 in several versions. Because the bare capsid is charged highly positively, the values of the potential range from −2 V to +25 V. The map was plotted using several scales, and only the scale, which was very strongly shifted towards the upper limit allowed to vaguely recognize the locations that are chloride-rich. We analysed two surfaces: the first is of the default thickness (determined by atomic radii of protein

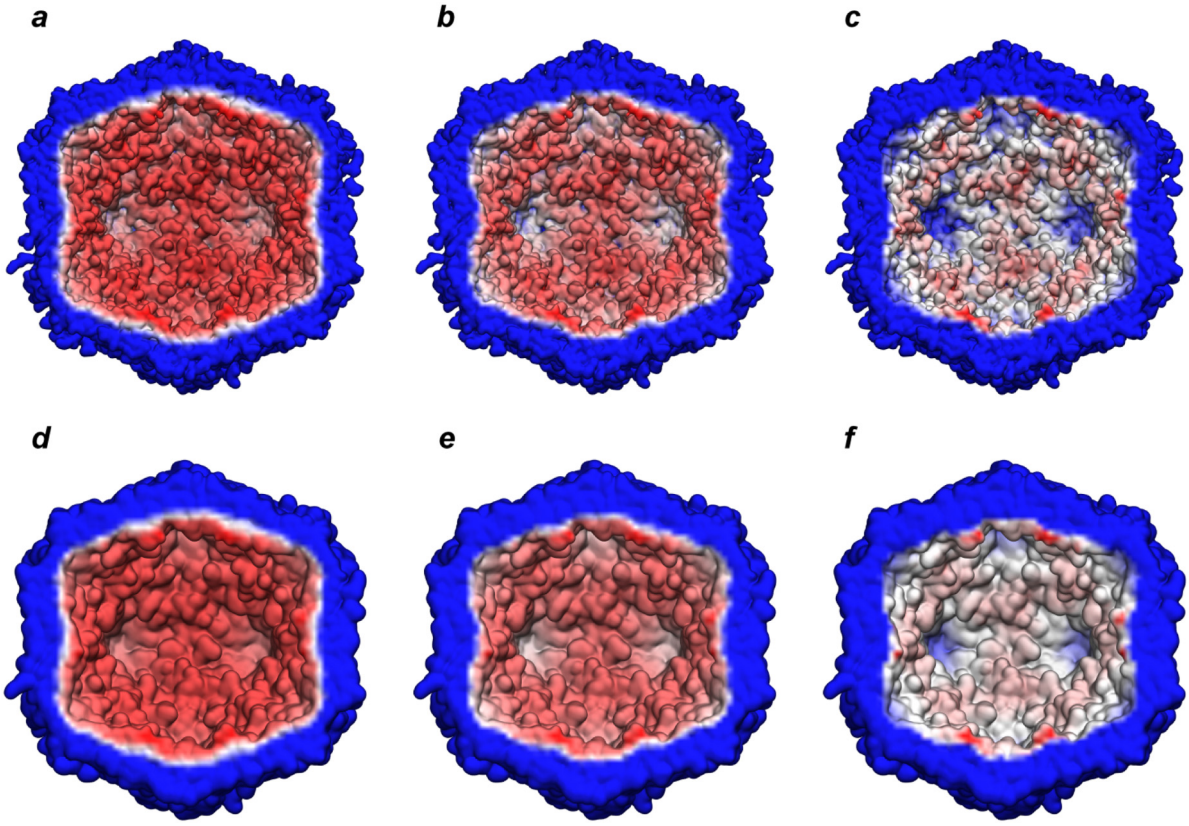

Fig. 7. Electrostatic potential maps of the capsid interior; top row: the capsid surface, bottom row: the surface at approximately 5 Å from the capsid; the scale ranges 13.7–23 V (a, d); 17–23 V (b, e); 20–23 V (c, f) with blue corresponding to the lower limit and red corresponding to the upper limit of the scale. (For interpretation of the references to color in this figure legend, the reader is referred to the web version of this article.)

atoms), and the second is at the distance of approximately 5 Å from the atoms and thus roughly corresponds to the surface where the ions are located. The insignificant variation of the electrostatic potential means that the distribution of the ions that we observe is hard to explain by the charges on the residues alone. A complicated interplay between the attraction by the charges on the amino acids and steric effects involving water and counter-ions plays the role.

4. Conclusions

The distribution of the chloride ions could mimic the localisation of the phosphate groups of the DNA/RNA as it was shown in [12] for a different virus. Because of the findings presented below, that could also have biological consequences that the stability of the capsid could be defined by a specific placement of the DNA chain.

In this work we have performed the comparison of two systems which were different only in the number of the ions inside the capsid, and the detailed analysis of the local ion distribution on the inner surface of the capsid's wall with the aim to identify how the ions distribution influences the capsid's stability.

We have found several amino acids that are highly attractive for the chloride ions in the capsid, and they are the same for both systems. Interestingly, the distribution of the electrostatic potential created by the capsid atoms across the capsid inner surface does not explicitly indicate the preferential binding places for the Cl^- ions.

We have found the amino acids which are occupied with chloride ions in NS, however, they have much less (almost zero) chloride ions in AS. As these amino acids are placed at the cracks in AS, we hypothesise that the deficit of the chloride ions close to these amino acids could cause the appearance of the cracks in the capsid and further deformation of the capsid structure that could lead to its collapse. Therefore, we suggest a hypothesis that these amino acids should interact with the negative charge of the chloride ions or the phosphate groups of the genome. In future research we will verify this hypothesis.

Supplementary data to this article can be found online at https://doi.org/10.1016/j.molliq.2018.06.019.

Acknowledgement

E.T. is a JSPS International Research Fellow, grant number PE17023; V. F. acknowledges the support of the Ministry of Education and Science of Ukraine, grant number 0117U004966; D.N. acknowledges the support of JSPS through BRIDGE Fellowship, grant number BR170303.

References

[1] E. Tarasova, I. Korotkin, V. Farafonov, S. Karabasov, D. Nerukh, Complete virus capsid at all-atom resolution: simulations using molecular dynamics and hybrid molecular dynamics/hydrodynamics methods reveal semipermeable membrane function, J. Mol. Liq. 245 (2017) 109–114.
[2] P.L. Freddolino, A.S. Arkhipov, S.B. Larson, A. McPherson, K. Schulten, Molecular dynamics simulations of the complete satellite tobacco mosaic virus, Structure 14 (3) (2006) 437–449.
[3] J.A. Roberts, M.J. Kuiper, B.R. Thorley, P.M. Smooker, A. Hung, Investigation of a predicted N-terminal amphipathic α-helix using atomistic molecular dynamics simulation of a complete prototype poliovirus virion, J. Mol. Graph. Model. 38 (2012) 165–173.
[4] Y. Andoh, N. Yoshii, A. Yamada, K. Fujimoto, H. Kojima, K. Mizutani, A. Nakagawa, A. Nomoto, S. Okazaki, All-atom molecular dynamics calculation study of entire poliovirus empty capsids in solution, J. Chem. Phys. 141 (16) (2014).
[5] D.S.D. Larsson, L. Liljas, D. van der Spoel, Virus capsid dissolution studied by microsecond molecular dynamics simulations, PLoS Comput. Biol. 8 (5) (2012) 1–8.
[6] E. Tarasova, V. Farafonov, R. Khayat, N. Okimoto, T.S. Komatsu, M. Taiji, D. Nerukh, All-atom molecular dynamics simulations of entire virus capsid reveal the role of ion distribution in Capsid's stability, J. Phys. Chem. Lett. 8 (2017) 779–784.
[7] Y. Zeng, S.B. Larson, C.E. Heitsch, A. McPherson, S.C. Harvey, A model for the structure of satellite tobacco mosaic virus, J. Struct. Biol. 180 (1) (2012) 110–116.
[8] M. Zink, H. Grubmüller, Mechanical properties of the icosahedral shell of southern bean mosaic virus: a molecular dynamics study, Biophys. J. 94 (4) (2009) 1350–1363.

[9] J.A. Speir, S. Munshi, G. Wang, T.S. Baker, J.E. Johnson, Structures of the native and swollen forms of cowpea chlorotic mottle virus determined by X-ray crystallography and cryo-electron microscopy, Structure 3 (1) (1995) 63–78.
[10] T.A. Jones, L. Liljas, Structure of satellite tobacco necrosis virus after crystallographic refinement at 2.5 Å resolution, J. Mol. Biol. 177 (4) (1984) 735–767.
[11] Y. Miao, J.E. Johnson, P.J. Ortoleva, All-atom multiscale simulation of cowpea chlorotic mottle virus capsid swelling, J. Phys. Chem. B 114 (34) (2010) 11181–11195.
[12] D.S.D. Larsson, D. Van Der Spoel, Screening for the Location of RNA Using the Chloride ion Distribution in Simulations of Virus Capsids, 8, 7, 2012 2474–2483.
[13] R. Khayat, N. Brunn, J.A. Speir, J.M. Hardham, R.G. Ankenbauer, A. Schneemann, J.E. Johnson, The 2.3-angstrom structure of porcine circovirus 2, J. Virol. 85 (15) (2011) 7856–7862.
[14] N. Wang, Y. Zhan, A. Wang, L. Zhang, R. Khayat, Y. Yang, In silico analysis of surface structure variation of PCV2 capsid resulting from loop mutations of its capsid protein (Cap), J. Gen. Virol. 97 (2016) 3331–3344.
[15] The Protein Data Bank. H.M. Berman, J. Westbrook, Z. Feng, G. Gilliland, T.N. Bhat, H. Weissig, I.N. Shindyalov, P.E. Bourne, Nucleic Acids Res. 28 (2000) 235–242.
[16] VIPERdb2: an enhanced and Web API enabled relational database for structural virology, Nucleic Acids Res. 37 (2009) D436–D442.
[17] B. Hess, C. Kutzner, D. van der Spoel, E. Lindahl, GROMACS 4: algorithms for highly efficient, load balanced, and scalable molecular simulations, J. Chem. Theory Comput. 4 (2008) 435–447.
[18] D. Van Der Spoel, E. Lindahl, B. Hess, G. Groenhof, A.E. Mark, H.J.C. Berendsen, GROMACS: fast, flexible, and free, J. Comput. Chem. 26 (16) (2005) 1701–1718.
[19] W. Humphrey, A. Dalke, K. Schulten, VMD - visual molecular dynamics, J. Mol. Graph. 14 (1996) 33–38.
[20] N.A. Baker, D. Sept, S. Joseph, M.J. Holst, J.A. McCammon, Electrostatics of nanosystems: application to microtubules and the ribosome, Proc. Natl. Acad. Sci. U. S. A. 98 (2001) 10037–10041.